Construction and Building Materials 121 (2016) 507–518

Contents lists available at ScienceDirect

Construction and Building Materials

journal homepage: www.elsevier.com/locate/conbuildmat

Influence of technological and environmental factors on the behaviour of the reinforcement anchorage zone of prestressed concrete sleepers

Aidas Jokūbaitis *, Gediminas Marčiukaitis, Juozas Valivonis

Department of Reinforced Concrete and Masonry Structures, Vilnius Gediminas Technical University, Sauletekio ave 11, LT-10223 Vilnius, Lithuania

HIGHLIGHTS

- Forces acting in prestressed concrete elements during heat treatment and reinforcement release.
- Comparison of experimental and calculated results of prestress force after heat treatment.
- Investigation of environmental impacts on concrete structure of sleepers.
- Analysis of concrete microstructure of new and damaged prestressed concrete sleepers.

ARTICLE INFO

Article history:
Received 19 January 2016
Received in revised form 19 May 2016
Accepted 11 June 2016
Available online 17 June 2016

Keywords:
Prestressed concrete
Technological factors
Concrete structure
Sleeper
SEM
EDS
DEF

ABSTRACT

The article analyses the influence of technological factors on variations in the stress and strain state during the production of prestressed concrete sleepers. The paper focuses on technological damage to the anchorage zone and its influence on concrete and the pretensioned reinforcement of the last prestressed concrete sleepers located by abutments. The article presents the calculation principles of stresses caused by thermal and humidity deformations, compares theoretical and experimental results and specifies the nature of damages. The paper deals with concrete structure and an interface between reinforcement and concrete of new and three years old prestressed concrete sleepers, explores the results of laboratory tests on deteriorating the ends of new prestressed concrete sleepers under freezing and thawing cycles, looks at changes in concrete structure and the interface between reinforcement and concrete at the ends and in the middle of prestressed concrete sleepers applying a scanning electron microscope (SEM) and energy-dispersive X-ray spectroscopy (EDS). Secondary ettringite formation (DEF) in concrete micro-cracks and at the interface between reinforcement and concrete and elemental composition of the formed crystals have been determined. Significant difference in concrete structure and new solid phases at the ends of used and new sleepers has been defined. Concrete structure in the middle of the three years old railway sleeper has remained almost unchanged. The obtained results show that technological factors are affecting the deterioration nature of the ends of prestressed concrete sleepers.

1. Introduction

Prestressed concrete structures are the ones of the most effective structures used for the buildings of various purposes and complexity. Prior to exploitation, prestressed concrete structures are affected by various technological factors appearing during production. The micro-cracking of concrete structure, initial stresses and strains in reinforcement and concrete appearing during the production of prestressed concrete structures are more dangerous comparing with ordinary reinforced concrete structures.

Concrete cracking at the reinforcement anchorage zone and damage to bond between reinforcement and concrete are induced by stress variations in pretensioned reinforcement during the production of prestressed concrete structures [1–4]. The conducted research [5] shows that bond between reinforcement and concrete depends on many technological factors: concrete composition and strength during reinforcement release, curing conditions, element maintenance after concrete design strength is reached, the type of reinforcement, and the methods of release. Other research [6,7] shows that variations in technological stresses in concrete and reinforcement are different and causes initial damage to concrete structure during production processes. Micro-cracks, open pores, capillary, bond damage between reinforcement and concrete during reinforcement release and other damages enable aggressive substances from the environment penetrate into concrete. Different chemical processes taking place in the micro-cracks and pores of concrete are induced by these damages. New solid phases

* Corresponding author.
E-mail address: aidas.jokubaitis@vgtu.lt (A. Jokūbaitis).

http://dx.doi.org/10.1016/j.conbuildmat.2016.06.025
0950-0618/

occurring in concrete micro-cracks and other imperfections cause additional stresses and can damage concrete structure [8–13].

The prestressed concrete elements of transport structures are affected by the greatest variety of effects. Extremely complicated environmental conditions influence prestressed concrete railway sleepers in service. Eight main reasons causing a failure in different types of the sleepers made from different materials are provided in a comprehensive analysis [14] of deteriorating prestressed concrete sleepers. Technological factors are one of the reasons, nevertheless, no more detailed research has been done. However, a number of studies on the behaviour of prestressed concrete sleepers under mechanical loads [15–20] and environmental conditions have been carried out and included a change in temperature [20], humidity and sulphate attack (delayed formation of ettringite) [12,22,23]. The behaviour and durability of the sleepers are affected by soil and ballast [24,25].

The performed research [10,21,22], shows that concrete corrosion and deterioration of prestressed concrete sleepers in service are highly dependent on the porosity of concrete structure and micro-cracks induced during production. Concrete structure and permeability have a significant impact on durability [26], bond between reinforcement and concrete, frost resistance and chemical (sulphate, alkaline) corrosion. An oxide layer can form on the surface of reinforcement before the production of reinforced concrete elements and it is dependant on the environmental conditions [27]. Therefore, oxide layer results a more hydrophilic surface and can enhance bond properties between reinforcement and concrete [28,29].

Different sources [15,22,23] show that the most common part of the damage and deterioration of prestressed concrete sleepers used in the natural environment are observed at their ends (reinforcement anchorage zone) (Fig. 1). This can be caused by the impact of water and frost [21], alkaline corrosion [23], sulphate corrosion [10,12,22] or concrete micro-cracking [9].

However, little research on the influence of technological factors on concrete porosity as well as on the appearance and development of micro-cracks during the entire period of production and service has been done. This work presents investigation of technological damages and their influence on construction behaviour during service. A qualitative influence of variations in the initial stress and strain state and bond between reinforcement and concrete on the behaviour of the reinforcement anchorage zone and construction quality has been analyzed.

2. Analysis of technological stresses and deformations of concrete and reinforcement

2.1. Influence of temperature on variations in stresses during production

An important point is ensuring the sufficient quality of technological processes during the production of prestressed concrete elements. However, this can be very hard to implement, because many complicated physical and chemical processes are happening between various materials and components in prestressed concrete elements. Technological damage to prestressed concrete elements is unavoidable because of different characteristics of materials and production processes. Reinforcement anchorage is the most important zone of prestressed concrete elements. Shear and normal stresses can cause the micro-cracking of concrete at the interface between concrete aggregate and cement paste, and reinforcement and concrete during heat curing of prestressed concrete elements.

Our analysis [6,30] and other authors examination [7,31] on technology for producing the prestressed concrete structure have revealed that the main production processes cause stress variation in reinforcement and concrete. In case of prestressing reinforcement to abutments, bond is forming between reinforcement and concrete at the beginning of concrete hardening. Bond strength depends on concrete composition, hardening conditions, maintenance after curing and the method of reinforcement release. The biggest change in stress is noticed in the part of reinforcement outside concrete at the end of the casting bed. When concrete is heated during production, shear stresses appear at the reinforcement and concrete interface due to difference in temperature. At this stage, stresses in reinforcement reduce due to reinforcement elongation. Compression force appears in concrete, because heated concrete expands and these deformations are restrained by bond between reinforcement and concrete. After hardening, during cooling, concrete shrinks and stresses in concrete decrease, but increase in reinforcement outside concrete due to different thermal and shrinkage deformations. Reinforcement is pulled out of concrete at the end of the last element and shear stresses appear at the interface between reinforcement and concrete. Reinforcement draws into concrete during release.

Fig. 2 describes technological effects at separate stages of production. The analysis of changing initial prestressing force P_0 shows that forces, in part of reinforcement outside concrete, cause stresses in the reinforcement anchorage zone and change its direction and value. Therefore, bond between reinforcement and concrete is more damaged at the end of the last element.

The first stages of prestressed concrete production include prestressing reinforcement to abutments (Fig. 2a), pouring concrete (Fig. 2b) and starting heat treatment. At these stages, opposite direction force F_1 (Fig. 2c) appears due to thermal deformations of reinforcement before bond between reinforcement and concrete appears. This force depends only on difference in temperature between abutments and the element. Then the total thermal deformation:

$$\Delta_{1(\Delta T)} = \alpha_p \cdot \Delta T_p (l_T - l_c) + \alpha_p \cdot \Delta T_c \cdot l_c, \quad (1)$$

where l_c is total length of prestressed concrete elements in casting bed; l_T heated part of casting bed; α_p thermal expansion coefficient

Fig. 1. End cracking of prestressed concrete sleepers.

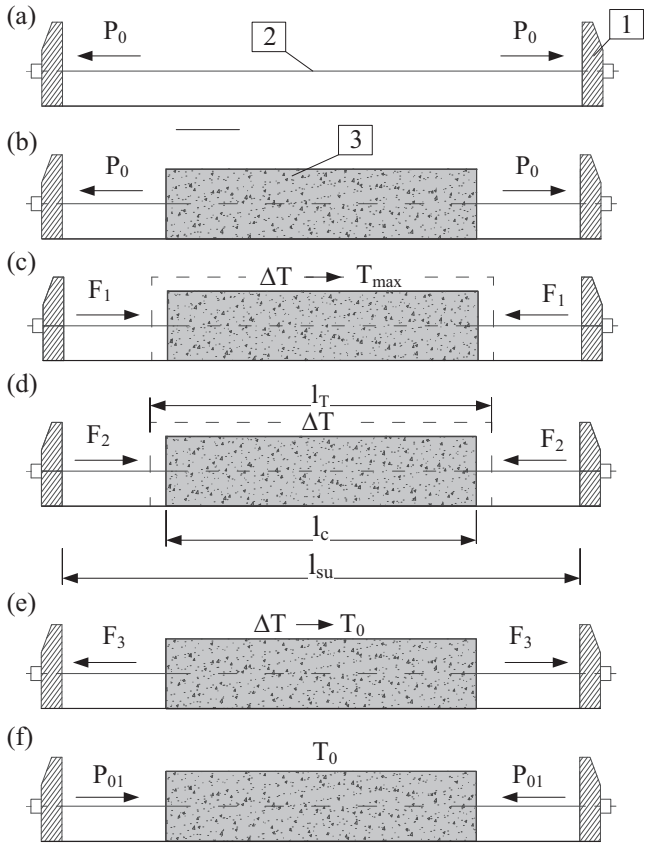

Fig. 2. Stages of prestress force variation during production: a – prestressing reinforcement (2) to the abutments (1); b – concreting (3) after maintenance; c – the beginning of heat treatment before bond between reinforcement and concrete appears; d – heat treatment ($\Delta T = T_{max} - T_0$); e – cooling stage (until T_0 or ambient); f – release of reinforcement.

of pretensioned reinforcement; ΔT_p and ΔT_c temperature difference in reinforcement outside and inside the concrete respectively.

Deformation δ_{11}

$$\delta_{11} = \frac{l_{su}}{E_p \cdot A_p}, \tag{2}$$

where l_{su} is distance between abutments; E_p modulus of elasticity of pretensioned reinforcement; A_p cross-sectional area of pretensioned reinforcement.

Expressing force F_1 from the equilibrium equation $\delta_{11} \cdot F_1 + \Delta_{1(\Delta T)} = 0$

$$F_1 = \frac{\Delta_{1(\Delta T)}}{\delta_{11}} = \frac{\alpha_p \cdot \Delta T_p (l_T - l_c) + \alpha_p \cdot \Delta T_c \cdot l_c}{l_{su}} \cdot E_p \cdot A_p, \tag{3}$$

Rearranging Eq. (3), when $\gamma_l = l_c/l_{su}$, $\lambda = l_T/l_{su}$, force F_1 can be calculated according to

$$F_1 = [\alpha_p \cdot \Delta T_p (\lambda - \gamma_l) + \alpha_p \cdot \Delta T_c \cdot \gamma_l] \cdot E_p \cdot A_p, \tag{4}$$

Bond strength between reinforcement and concrete reaches the stage at which free deformation of reinforcement is restrained during heat treatment. At this stage full bond between reinforcement and concrete develops. Reinforcement and concrete start acting as one structure, and thermal and other deformations are equal at the reinforcement level. Then it is assumed that $F_1 = F_2$ and $\Delta T_p = \Delta T_c$ and total thermal deformation

$$\Delta_{1(\Delta T)} = \alpha_p \cdot \Delta T_p \cdot (l_T - l_c) + \alpha_c \cdot \Delta T_c \cdot l_c, \tag{5}$$

Deformation δ_{11}

$$\delta_{11} = \frac{(l_{su} - l_c) + 2 \cdot l_{eff.p}}{E_p \cdot A_p} + \frac{l_c - 2 \cdot l_{eff.p}}{E_p \cdot A_{c.eff}}, \tag{6}$$

where $l_{eff.p}$ is effective anchorage length of reinforcement; $A_{c.eff}$ effective cross-section area of prestressed concrete element.

Changes in temperature ($\Delta T = T_{max} - T_0$) appear between abutments and pretensioned reinforcement outside concrete during heat treatment. Because of an increase in temperature, the opposite direction force appears in reinforcement outside concrete, which reduces the initial prestressing force (Fig. 2d). Force in reinforcement outside concrete can be calculated rearranging Eqs. (5) and (6)

$$F_2 = \frac{[\alpha_p \cdot \Delta T_p (\lambda - \gamma_l) + \alpha_c \cdot \Delta T_c \cdot \gamma_l] \cdot E_p \cdot A_p}{D}, \tag{7}$$

where $D = 1 - \gamma_l/(1 + \rho \cdot \alpha_0)$; ρ reinforcement ratio: $\rho = A_p/A_c$; α_0 ratio between modulus of elasticity of pretensioned reinforcement and concrete: $\alpha_0 = E_p/E_c$; α_p and α_c thermal expansion coefficient of pretensioned reinforcement and concrete respectively.

During heat treatment, the highest temperature is maintained for a certain period of time, and after, the cooling stage starts (Fig. 2e). Within the process of cooling prestressed concrete elements, additional tension force appears in reinforcement outside concrete, as it tries to regain its initial position. According to Eq. (7), reinforcement pull out force during cooling of prestressed concrete element can be calculated as

$$F_3 = \frac{F_1}{D} = \frac{[\alpha_p \cdot \Delta T_p \cdot (\lambda - \gamma_l)] \cdot E_p \cdot A_p}{1 - \frac{\gamma_l}{1 + \rho \cdot \alpha_1}}, \tag{8}$$

where $\alpha_1 = E_{p1}/E_{c1}$ is ratio between modulus of elasticity of reinforcement and concrete during cooling stage.

Reinforcement outside concrete is affected by additional tension force because of concrete shrinkage during cooling, and this force can be calculated according to the equation

$$F_{sh} = \frac{\varepsilon_{sh} \cdot E_p \cdot A_p \cdot \gamma_l}{1 - \frac{\gamma_l}{1 + \rho \cdot \alpha_{01}}}, \tag{9}$$

where ε_{sh} is total shrinkage strain of concrete during cooling: $\varepsilon_{sh} = \varepsilon_{c.sh} + \varepsilon_{T.sh} + \varepsilon_c$; $\varepsilon_{c.sh}$, $\varepsilon_{T.sh}$ and ε_c drying shrinkage strain, thermal shrinkage strain and autogenous shrinkage strain of concrete respectively.

Total additional force in pretensioned reinforcement outside concrete after heat treatment due to technological factors:

$$F = F_3 + F_{sh} - F_2 - F_1, \tag{10}$$

Then total prestressing force in reinforcement outside concrete:

$$P_{01} = P_0 + F, \tag{11}$$

An increase of reinforcement prestress force will have a negative impact on the prestressed concrete anchorage zone during the release of reinforcement. Reinforcement slip and transfer length will increase at the end of the prestressed concrete element because of an increase in prestress force. Larger cracks will appear around reinforcement and at the interface between reinforcement and concrete.

Experimental research on prestress losses in prestressed concrete railway sleepers during heat treatment was performed in the factories in Lithuania and Sweden [32,33]. Variations in the prestress force of reinforcement outside and inside concrete were determined during experimental research, depending on temperature mode. At first, reinforcement is prestressed to rigid abutments maintained for 3 h, and then, concrete is poured. Reinforcement deforms freely until bond between reinforcement and concrete appears when the curves of prestress force in

reinforcement outside and inside concrete start deviating (Fig. 3). At this stage, reinforcement deformations are restrained by concrete. At the highest temperature during heat treatment, concrete strength is reached at which full bond between reinforcement and concrete appears (Fig. 3). Tension force is induced in reinforcement outside concrete by concrete shrinkage during cooling prestressed concrete elements. Reinforcement was released after 21 h when concrete was not fully cooled down in the factory in Lithuania, and prestress force in reinforcement outside concrete increased about 3%. Meanwhile, in the factory in Sweden, reinforcement was released after 66 h when concrete was fully cooled down and prestress force in reinforcement outside concrete increased about 15%. Prestress force before reinforcement release was estimated according to the proposed calculation methodology (Eqs. (4), (7), (8), (9)) of additional force in reinforcement outside concrete (Fig. 3). Theoretically calculated prestress forces in reinforcement outside concrete in the factories in Lithuania and Sweden are 6% lower and 8% higher than the initial prestress forces respectively.

The performed theoretical analysis has disclosed that variations in prestress force during heat treatment mainly depend on difference in temperature (ΔT) and ratio (γ_l) between the total length of prestressed concrete elements in the casting bed and the distance between abutments (Fig. 4). The shorter is the reinforcement outside concrete, the higher deformations will appear in this part of reinforcement, and prestress force will increase before release.

Experimental research [7,30] has showed that prestress force is lower if reinforcement is released when concrete is not fully cooled down. Prestress force significantly increased during reinforcement release when concrete was fully cooled down.

2.2. Influence of reinforcement release order on stress variation

There are several methods of reinforcement release: sudden and gradual. Reinforcement can be released simultaneously or in sequence. The conducted research has showed that the order of pretensioned reinforcement release affects the reinforcement anchorage zone. End cracking of prestressed concrete elements can occur due to an inappropriate order or method of reinforcement release [1–3]. When reinforcement is released in sequence, prestress force redistributes between unreleased prestressed reinforcing bars (Fig. 6). After releasing one reinforcing bar (Fig. 6b), the initial prestress force is taken over by the remaining unreleased reinforcing bars. Consequently, tension force increases in every unreleased reinforcing bar. Tension force will also increase in remaining unreleased reinforcing bars during the release of other reinforcement. Variations in tension force depend on the method of reinforcement release and sequence.

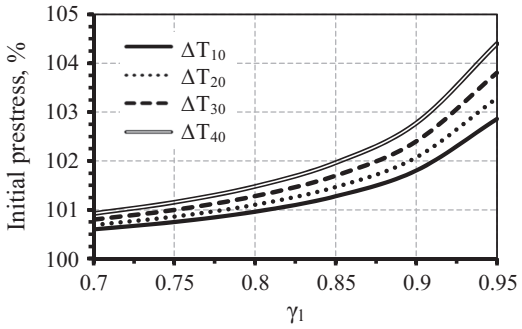

Fig. 4. Initial prestress in pretensioned reinforcement outside the concrete after heat treatment.

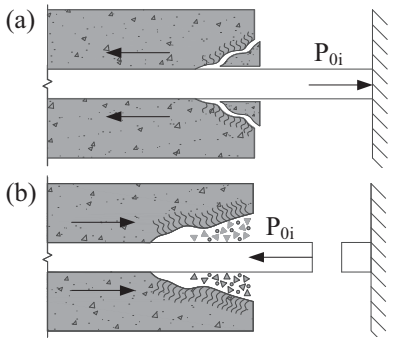

Fig. 5. Initial anchorage zone damage: a – due to concrete shrinkage and temperature change before reinforcement release; b – due to reinforcement release.

Before and after reinforcement release, a different stress and strain state appears during the production of prestressed concrete elements. Unreleased prestressed reinforcement outside concrete is pulled out of concrete due to concrete shrinkage and different thermal deformations of reinforcement and concrete. The end surface of the prestressed concrete element deforms around reinforcement because the latter is pulled out of concrete (Fig. 5a). Tensile strain appears in concrete around the reinforcing bar before reinforcement release and concrete plain around reinforcement deforms.

Tensile and shear stresses appear at the interface between reinforcement and concrete and the damaged area around reinforcement and damaged anchorage length increases after reinforcement release (Fig. 5b). Reinforcement draws in deeper into concrete due to the initial concrete damage around reinforcement during release. Stress redistribution takes place in the reinforcement

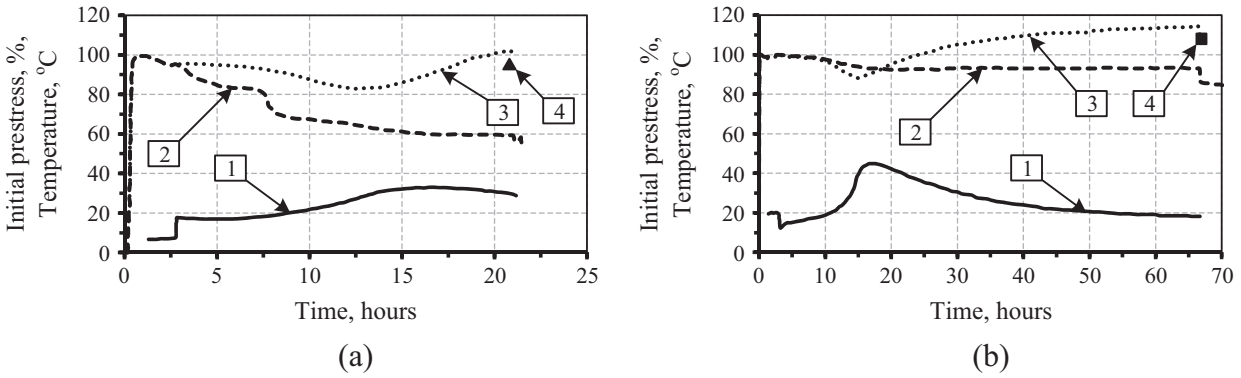

Fig. 3. Variation of prestress in reinforcement inside and outside the concrete and concrete temperature in the factories in Lithuania (LTU) a) and Sweden (SWE) b): 1 – temperature; 2 – prestress force inside concrete; 3 – prestress force outside concrete; 4 – theoretical prestress force outside concrete.

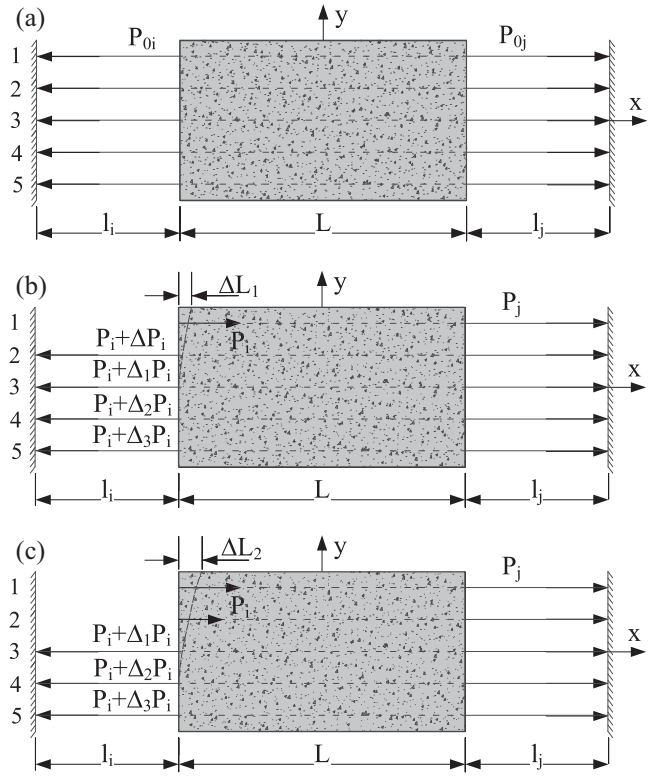

Fig. 6. Redistribution of prestress force during sequential release of reinforcement.

anchorage zone. Reinforcement draw in varies due to the release of reinforcement in sequence (Fig. 6c). This can be explained by variation in damage to the reinforcement anchorage zone.

After releasing several reinforcing bars, prestress force acting in each unreleased bar can be calculated according to [6,7]

$$P_i = [P_0 - (s_x - s_i) \cdot k_i], \tag{12}$$

$$P_j = [P_0 - (s_x - s_j) \cdot k_j], \tag{13}$$

where P_i and P_j are forces at the active and passive end of casting bed respectively; P_0 initial prestress force before reinforcement release; s_x displacement of prestressed concrete elements along the axis of casting bed due to reinforcement release; s_i and s_j component of longitudinal compressive strain of prestressed concrete elements due to concrete precompression during release of reinforcement at active and passive end of the casting bed respectively; k_i and k_j coefficients describing reinforcement axial tensile stiffness depending on anchorage zone length from active and passive end of casting bed respectively.

Displacement of prestressed concrete element along the axis of casting bed

$$s_x = \frac{[(m-n) \cdot P_0 - R \cdot F_{fr}]}{(p-m) \cdot k_i + (p-n) \cdot k_i}, \tag{14}$$

where F_{fr} is friction force appearing when prestressed concrete element tries to move along the casting bed: $F_{fr} = m_e \cdot g \cdot \mu$; m_e mass of the elements; g acceleration of gravity ($g = 9.81\ \mathrm{m/s^2}$); μ coefficient of friction (steel to concrete $\mu = 0.57 \ldots 0.7$ [34]); p amount of all prestressed reinforcing bars in cross-section; m and n amount of released reinforcing bars at active and passive end of the casting bed respectively; R coefficient of restraint degree.

The ratio between element length and cross-section height is an important factor describing movement along the casting bed. The longer is the element, comparing with the height of its cross-section, the greater is the degree of restrain (R). When an element is free to move and is completely unrestrained, $R = 0$. In case of partial restrain, $0 < R < 1$ and in case of full restrain, $R = 1$. Calculations are done assuming that abutments are rigid and cannot deform. Usually reinforced concrete elements are long comparing to the height of their cross-section and cannot move along the axis, so $R = 1$.

Displacement of prestressed concrete element induced by precompression force:

$$s_i = \frac{m \cdot P_0 - (p-m) \cdot k_i \cdot s_x}{k_c \cdot (1+a) + (p-m) \cdot k_i}, \tag{15}$$

$$s_j = a \cdot \frac{m \cdot P_0 - (p-m) \cdot k_i \cdot s_x}{k_c \cdot (1+a) + (p-m) \cdot k_i}, \tag{16}$$

where $a = (p-m) \cdot k_i / p \cdot k_j$; $k_{i,j} = E_p \cdot A_p / l_{i,j}$; $l_{i,j} = l_{0i,j} + 0.5 \cdot l_{ai,j}$; l_{0i} and l_{0j} is reinforcement length outside the concrete at the active and passive end of casting bed respectively; l_{ai} and l_{aj} is reinforcement anchorage length at the active and passive end of casting bed during reinforcement release respectively; k_c stiffness coefficient of prestressed concrete element during concrete precompression: $k_c = (E_c \cdot A_c + E_p \cdot A_p)/(L - 0.5 \cdot (l_{ai} + l_{aj}))$; L total length of prestressed concrete elements in casting bed.

The analysis of the symmetrically released reinforcement of a prestressed concrete sleeper was performed according to the presented methodology (Eqs. (12)–(16)) and the initial data are presented in Table 1. It is assumed that pretensioned reinforcement is released symmetrically (Fig. 7a). Stress distribution in reinforcement depending on the ratio between the amount of released strands and a total amount of strands in the cross-section (m/p) and $\gamma_l = 0.7 \ldots 0.99$ is presented in Fig. 7b. Bond between reinforcement and concrete is the most damaged during the release of the last strands. The last strands can reach yielding stress or even brake due to an increase in prestress force during release.

3. Experimental research on damage to the reinforcement anchorage zone in prestressed concrete sleepers

3.1. Used materials and their properties

For investigation of the damaged ends of prestressed concrete sleepers, after reinforcement release, new (stored in warehouse) sleepers and those used for three years in the railroad track were used. Both used and new sleepers were produced at the same time in Lithuania and exploited in neighbouring countries (Fig. 8).

Concrete cubes ($100 \times 100 \times 100$ mm) were cut from new sleepers and the average concrete compressive strength was determined and made $f_{c,cube} = 80.6$ MPa. Concrete porosity by water absorption was 3.3%. The composition of the concrete mixture is given in Table 2.

Investigation of resistance to alkaline corrosion was made according to RILEM TC 191-ARP [35] and tested whether there were reactive particles in aggregate. Granite was used as a coarse aggregate for producing sleepers, which experimentally was determined as nonreactive filler. Therefore, the RILEM method [36], which includes small size (04 mm) aggregates, was selected for the expansion test.

Table 1
Initial data.

E_p, (GPa)	E_{c0}, (GPa)	f_{pk}, (MPa)	$f_{pk0,1}$, (MPa)	σ_0, (MPa)
195	31	1860	1674	1354
A_p, (mm^2)	A_c, (mm^2)	l_{su}, (m)	l_T, (m)	$\alpha_c = \alpha_p$
280.6	35,610	100	98	$10 \cdot 10^{-6}$

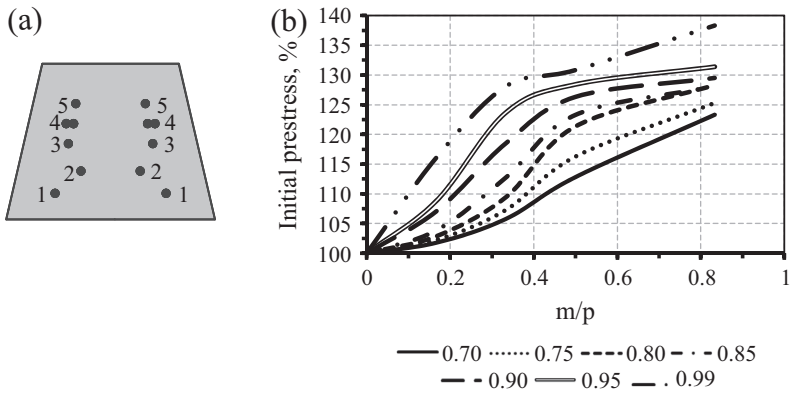

Fig. 7. a) Cross-section of rail seat and the order of reinforcement release, b) variation of initial prestress during sequential reinforcement release.

Fig. 8. Used prestressed concrete sleepers.

Alkali content in cement was determined according to LST EN 196-2:2013 [37] and was equal to $K_2O = 0.96\%$; $Na_2O = 0.13\%$; ($\%Na_2O_{eq} = Na_2O + 0.658\ \%K_2O$) $Na_2O_{eq} = 0.76\%$. Alkali content higher than 3.8 kg/m^3 causes destructive expansion and 1.8 kg/m^3 Na_2O_{eq} is the safe limit [38]. However, when alkali content in concrete is lower than 3 kg/m^3, it is assumed that alkaline corrosion in concrete cannot progress [39,40]. The equivalent amount of alkali content Na_2O_{ekv} in cement used in our research, is 2.89 < 3 kg/m^3. In many countries using lower alkalinity cement (low <0.6%; average >0.6%, <0.75%; high >0.75%) [39,40] is recommended for producing prestressed concrete sleepers.

Alkali content in concrete depends on the alkalinity of aggregates and cement, their content and ratio. According to laboratory tests, the amount of reactive particles in coarse aggregate (granite) is low [41]: the amount of highly reactive particles is 0.64% and the amount of lower reactivity particles is 0.62%. The amount of highly reactive particles and lower reactivity particles in fine aggregate (sand) is 1.52% and 2.33% respectively. The total amount of reactive particles in sand is about 4% and in granite – about 1%. Therefore, expansion tests were performed using only sand as fine aggregate.

Table 2
Composition of concrete mixture.

Material name, grade, fraction		Dry matter content kg/1 m^3 in concrete
Cement	Portland cement CEM I 52.5 R	380
Fine aggregate	Sand fr. 0–4	773
Coarse aggregate	Granite fr. 5–8	406
	Granite fr. 11–16	754
Additives	Accelerating admixture	0.5%
	Air entrainer	0.57%
Water		140
Water-cement ratio W/C		0.37
Density of the concrete		2453

Expansion due to alkaline corrosion of two types concrete samples were tested. Prismatic specimens (40 × 40 × 160 mm) were formed from sand and cement in a ratio 2.25:1. Water and cement ratio was 0.47. Other tested specimens (40 × 40 × 160 mm) were cut from new sleepers and consisted of fine (sand) and coarse (granite) aggregate (Table 2). The samples were stored in the NaOH solution of 1 M concentration at a temperature of 80 °C.

According to [35] recommendations, if the expansion of concrete samples does not exceed 0.10% within 14 days, then, there is no risk of alkaline corrosion. According to graphical data presented in Fig. 9 all aggregates (their amount) in concrete, used for producing sleepers, does not cause a dangerous alkaline reaction.

It has been determined that the structure of concrete samples cut from sleepers and soaked in alkali solution is damaged and surface cracks after 46 days (Fig. 10b). However, there were no cracks on the concrete surface of alkali unaffected samples (Fig. 10a). Concrete prisms were tested under bending and the tensile strength of concrete prisms soaked in the alkali solution was determined to decrease about 2 times.

3.2. Damages at the ends of new and used sleepers

A number of authors [8,10,11,22], have proved that micro- and macro-cracking is the initial damage causing further destruction of the concrete structure. The article discusses technological factors in a negative impact on the ends of sleepers (reinforcement anchorage zone). Damage to the concrete structure and initial stresses appearing during production creates conditions for further and faster concrete deterioration during exploitation due to humidity, water, freezing and thawing cycles as well as by chemical and physical effects caused by the gas or liquid form of contaminants.

Investigation into the used sleepers has disclosed that their ends are damaged differently (Fig. 8). Some of them are slightly damaged and therefore cracking and spalling concrete at the other ends and the reinforcement anchorage zone is observed.

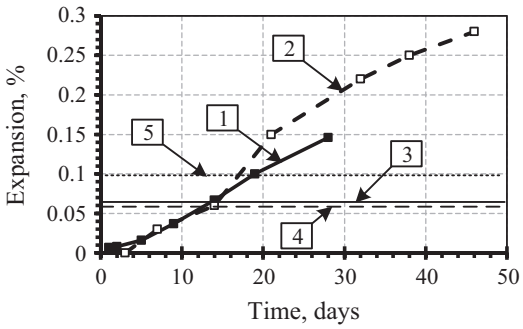

Fig. 9. Comparison of concrete expansion stored in 1 M concentration NaOH solution at 80 °C temperature: 1 – samples according to RILEM; 2 – samples from sleepers; 3 – expansion of samples according to RILEM after 14 days; 4 – expansion of samples from sleepers after 14 days; 5 – limit of expansion after 14 days (RILEM AAR-0).

A microscopic inspection of three years old used prestressed concrete sleepers having the damaged reinforcement anchorage zone was performed. Concrete damage and cracks around the reinforcement of the used sleepers is significantly larger (Fig. 11) than that viewed in new sleepers (stored in warehouse for three years) (Fig. 12). This shows that the initial damage to the concrete structure, caused by technological effects, increases during the exploitation of sleepers in the natural environment. The interface between reinforcement and concrete is damaged, and after reaching a certain level of cracking, concrete can split off and sleeper deterioration can begin. The first additional stresses in concrete are caused by water and humidity.

Water penetrates into micro- and macro-cracks on the concrete surface and causes stress in concrete and at the interface between reinforcement and concrete during freezing of water (Fig. 14). At the beginning of the crack, frozen water causes pressure to the surrounding concrete and unfrozen water is situated deeper in the crack. Unfrozen water creates hydraulic pressure at the tip of the crack and causes additional stress concentration. The interface between reinforcement and concrete can be damaged due to above introduced stresses. The further development of technological cracks or open pores, situated by reinforcement, is possible if cracks are filled with water to almost 95%. Unfrozen water helps with developing other chemical and physical processes in concrete micro-cracks (Fig. 14(5) and (6)). New solid expansive phases can form under wet conditions due to chemicals from the environment penetrating into concrete. New solid phases can cause large tensile stresses and damage concrete surface layers similarly as frozen water [42].

Experimental research on four new prestressed concrete sleepers under 200 freezing and thawing cycles was carried out. Each sleeper was cut in half before the test. This resulted into two sleeper end zones: a natural structural end and a sec-

Fig. 10. Concrete structure of samples from sleepers: a – before soaking in alkali solution; b – after soaking for 46 days.

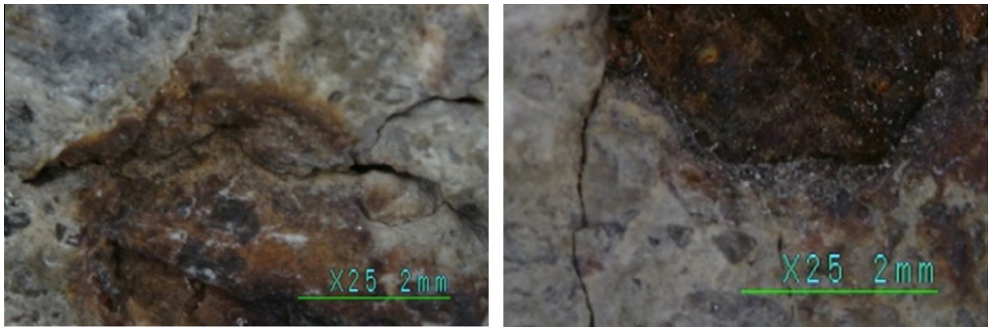

Fig. 11. Types of damage around reinforcement at the ends of three years old used sleepers.

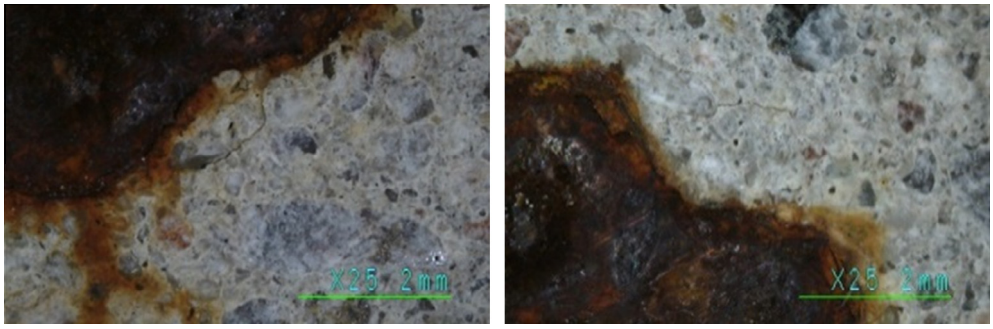

Fig. 12. Types of damage around reinforcement at the ends of new (stored in warehouse) sleepers.

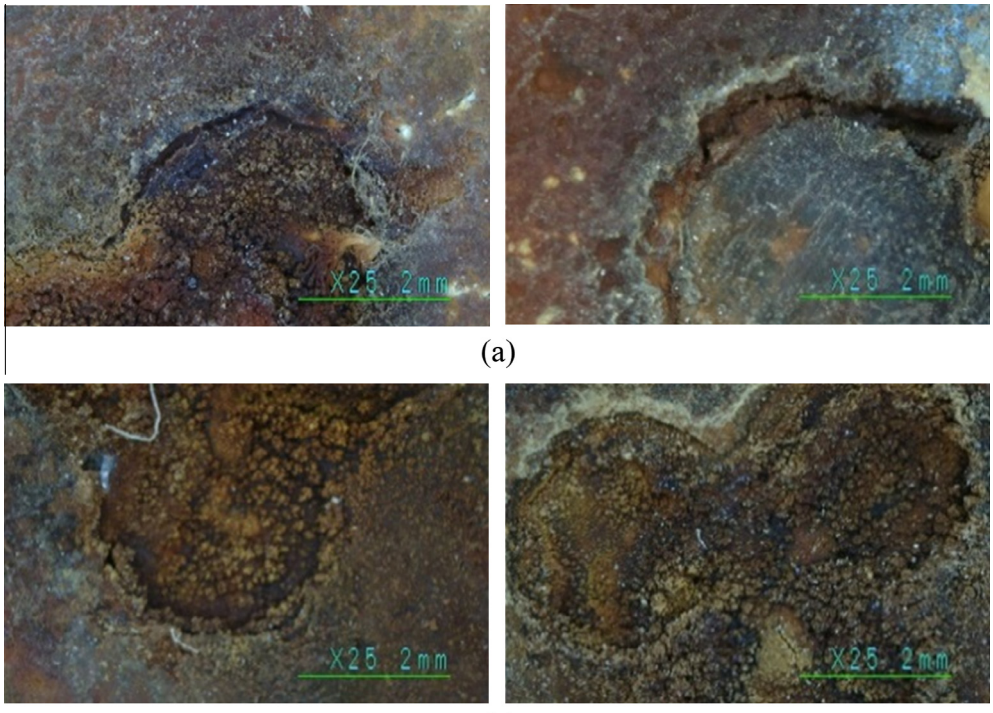

Fig. 13. Sleepers end surface after freezing and thawing: a) natural structural end; b) section in the middle of the sleeper.

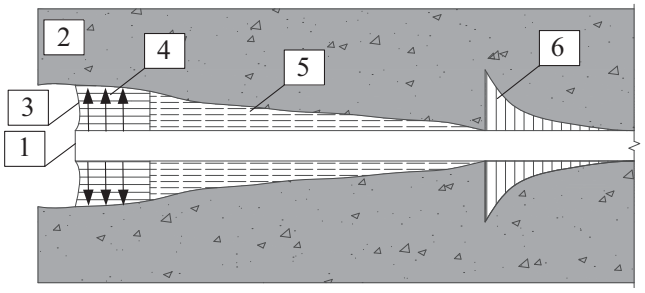

Fig. 14. Technological crack development during freezing of water: 1 – reinforcement; 2 – concrete; 3 – crack; 4 – frozen water (ice); 5 – unfrozen water; 6 – stress concentration due to pressure induced by frozen water.

tion in the middle of the sleeper. One freezing and thawing cycle lasted for 6–4 h of freezing (−17 °C) and 2 h of thawing in water (10 °C). At the end and in the middle of new sleepers, reinforcement was uncovered. The reinforcement surface was determined to be corroded up to 5 mm at the natural structural end and there was no corrosion of reinforcement in the middle of the sleeper. Sleepers were examined after freezing and thawing cycles, and concrete damage around reinforcement at the ends of sleepers was analysed (Fig. 13). A comparison of damage at the structural end of sleepers and the section in the middle of the sleeper shows that the interface between reinforcement and concrete is more damaged at the end of the sleeper due to technological damage during production (Fig. 13a). The reinforcement surface is corroded up to 23 mm at the structural end and up to 5 mm in the middle section of the sleeper. The middle section of the sleeper was affected only by the slip of prestressed reinforcement during cutting the sleeper. Therefore, damage to this area was smaller (Fig. 13b). This is confirmed by the influence of the initial stress state on the behaviour of prestressed concrete sleepers due to the exposure of humidity and temperature. Larger micro-cracks formed between reinforcement and concrete allow water to penetrate deeper into the concrete structure. These cracks create conditions for reinforcement corrosion, damage to the interface between reinforcement and concrete during freezing water and water presence in chemical processes during thawing.

Reinforcement was damaged by corrosion at the ends of the used sleepers where concrete was not spalled. Corrosion depth in some damaged reinforcement bars was up to 40 mm.

3.3. Analysis of sulphate attack

Concrete imperfections arising due to technological factors during production are unavoidable in almost all cementitious concrete. Their influence appears during the service of constructions. A further change in concrete structure and deterioration under acting loads as well as an environmental impact are influenced by open pores, capillaries, micro- and macro-cracks. One of the typical parts where deterioration starts in the case of our investigated sleepers and can be met in literature [12,22] are the ends of the sleepers, at which the biggest technological defects appear. According to Mehta [8], prestressed concrete sleepers deterioration mechanism can be divided into physical and chemical. The formation of new solid phases in concrete structure can cause chemical deterioration.

Sulphates and gypsum in cement rapidly dissolve during hydration, react with C_3A and ettringite forms. Ettringite formation, at the initial stage of concrete hardening, is called primary ettringite, which controls concrete curing time. Dangerous stresses do not appear during the formation of primary ettringite because cement paste is not hardened. After some time, the recrystallization of secondary ettringite ($3CaO{\cdot}Al_2O_3{\cdot}3CaSO_4{\cdot}32H_2O$) appears during service. An additional sulphate source (aqueous solution saturated with ions: Ca^{2+}, $Al(OH)_4^-$, SO_4^{2-} and OH^-), which can appear due to temperature effect or leaching alkalis in a humid environment, is required for the formation of secondary ettringite that forms due to internal sulphate attack (ISA), the development of which requires concrete micro-cracks, late sulphate release and water [10,11].

Ettringite usually forms on the concrete surface and is detected in concrete pores, cavities, cracks and micro-cracks around aggregates. Constructions, such as prestressed concrete sleepers, in service can be affected by a high temperature (>60 °C) during summer. Our researches and investigation done by other authors [12,14,22] have revealed that the deterioration of prestressed concrete sleepers used in railroad starts at their ends. The sleepers exposed to rainwater and variable effects of the sun are more damaged by internal sulphate attack than those constantly situated in the shadow and exposed to rainwater [10,43]. Our research also showed that more significant damages were detected at these ends of the sleepers situated on the south side and exposed to the sun, than ends of the sleepers situated on the northern side (Fig. 8).

Alkali silica reaction (ASR) accelerates the formation of secondary ettringite due to ISA. In case of reactive aggregates in concrete, alkali induced expansion occurs and micro-cracks appear in concrete during heat treatment. Ettringite forms in these micro-cracks and induces additional expansion and greater concrete cracking during hardening of concrete [44]. Secondary ettringite formation is also determined in concrete with nonreactive aggregates [10].

Thaumasite ($CaSiO_3{\cdot}CaCO_3{\cdot}CaSO_4{\cdot}15H_2O$) can form in cement and concrete containing carbonates. Calcium silicate (Ca_2SiO_4), sulphates, carbonates (limestone in cement, concrete aggregates, ground water, soil or CO_2 in air) and the excess of moisture are required for the formation of thaumasite.

Thaumasite can form from ettringite that reacts with C–S–H, carbonate, Ca^{2+} ions and water. In this case, a temperature lower than 15 °C (optimal 05 °C) is necessary for the formation of thaumasite [45]. At this temperature, reaction between ettringite, silicates (especially C–S–H) and carbonates (with CO_2^- ions or CO_2 in the atmosphere) takes place under the influence of water. Thaumasite crystals also form under a temperature higher than 20 °C, but the process takes longer [46]. However, formation of thaumasite can be faster in laboratory conditions [47].

It has been determined that an alkaline environment ($pH \geqslant 12.5$) accelerates the formation of thaumasite and that when water leaches various substances out of concrete at a low pH level ($pH \leqslant 8.0$), gypsum becomes dominant sulphate and the amount of thaumasite decreases. However, when thaumasite is completely formed, it remains stable even when the pH level is low and makes 68 [48].

It has been determined that thaumasite forms only in concrete containing enough sulphates, which would turn all aluminium into ettringite. Therefore, the presence of gypsum [49] or sulphates in the solution [50] can cause thaumasite formation in cement containing carbonates.

According to numerous studies [9,10,12,14,22], ettringite appears as one of the main factors in the sleeper deterioration process. According to the programme developed by the authors and selected specimens, the concrete structure of new and used prestressed concrete sleepers was investigated at the Laboratory of Building Products Technology in the Scientific Institute of Thermal Insulation, Vilnius Gediminas Technical University.

Concrete samples of testing were taken from different ends of the used, similarly damaged prestressed concrete sleepers (Fig. 1). Analyses employing a scanning electron microscope (SEM) and Energy-dispersive X-ray spectroscopy (EDS) were carried out at the interface (C) between aggregate (A) and cement paste (Fig. 15a). As the picture of microstructure analysis shows, the biggest changes arising from different humidity (shrinkage) and

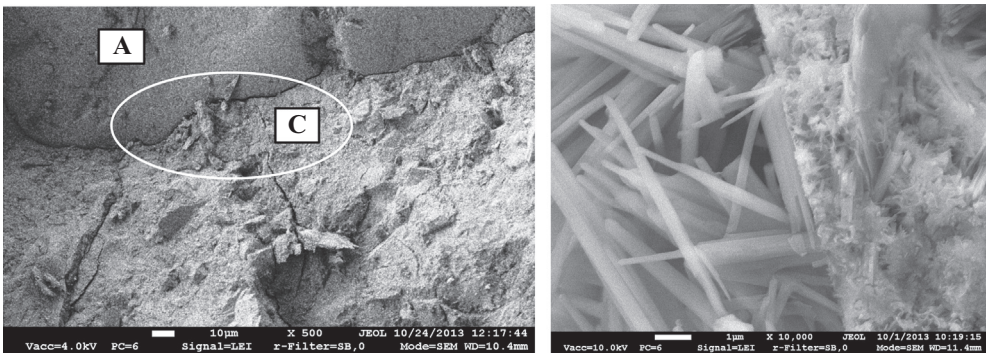

Fig. 15. Microstructure of specimen from the end of the used sleeper: a – ×500 (A – aggregate; C – contact zone); b – specimen from the C zone (×10,000).

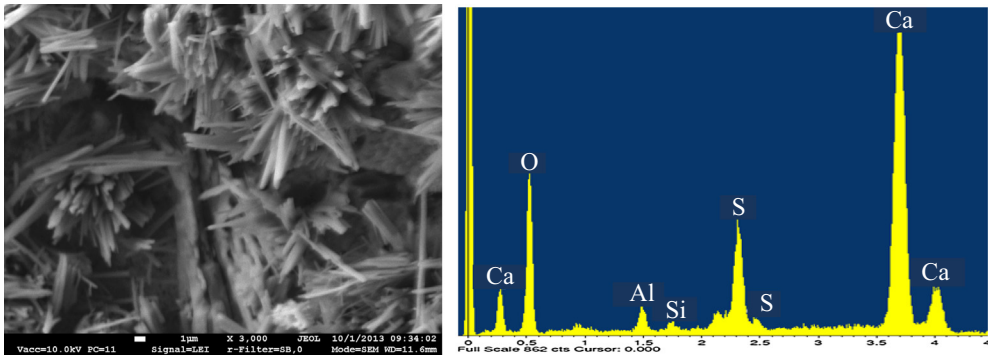

Fig. 16. Results of EDS analysis of the concrete specimen from the end of used sleeper: a – image of EDS analysis (×3000); b – results of element concentration (%): O – 28.30; Al – 3.88; Si – 0.25; S – 12.92; Ca – 54.65.

thermal deformations of these two components can be observed at the interface between aggregate and cement paste. More detailed research on this zone showed that all micro-cracks and pores were filled with various sizes of secondary ettringite (DEF) crystals, which causes internal stresses at the ends of sleepers.

EDS analysis along with SEM was carried out. Specimens from the ends of the used sleepers were taken in the parts between reinforcement and at the interface between reinforcement and concrete. The obtained results show that a significant amount of needle-shaped crystals formed in the micro-cracks of concrete at the interface between reinforcement and concrete (Fig. 17) and about 50 mm from reinforcement (Fig. 16). An elemental composition of these crystals corresponds to ettringite ($3CaO{\cdot}Al_2O_3{\cdot}3CaSO_4{\cdot}32H_2O$).

Secondary ettringite formation in concrete micro-cracks and pores shows that sulphate corrosion began at the ends of the used sleepers. Sulphate corrosion products were not observed in the structure of concrete specimens from the middle of the used sleepers (Fig. 18).

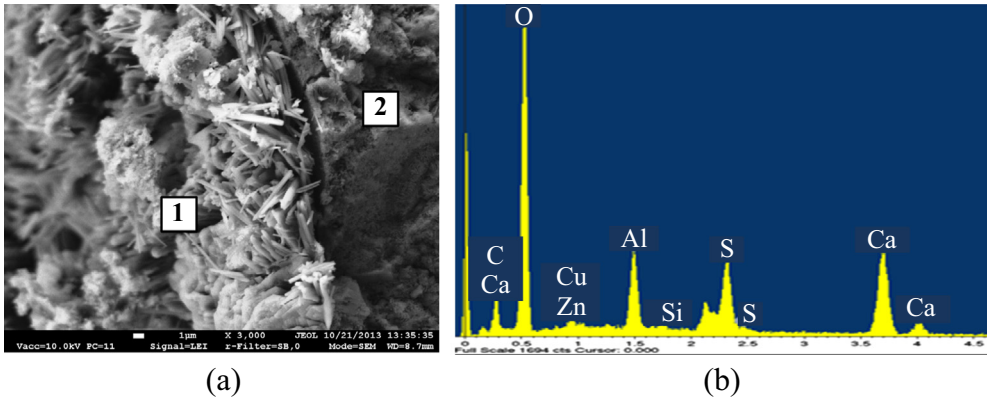

Fig. 17. Results of EDS analysis of specimen from the end of used sleeper at the interface between reinforcement and concrete: a – image of EDS analysis (×3000) (1 – interface between reinforcement and concrete; 2 – concrete), b – results of element concentration (%): O – 53.78; Al – 5.33; Si – 0.39; S – 7.94; Ca – 22.89; Cu – 2.33; C – 7.34.

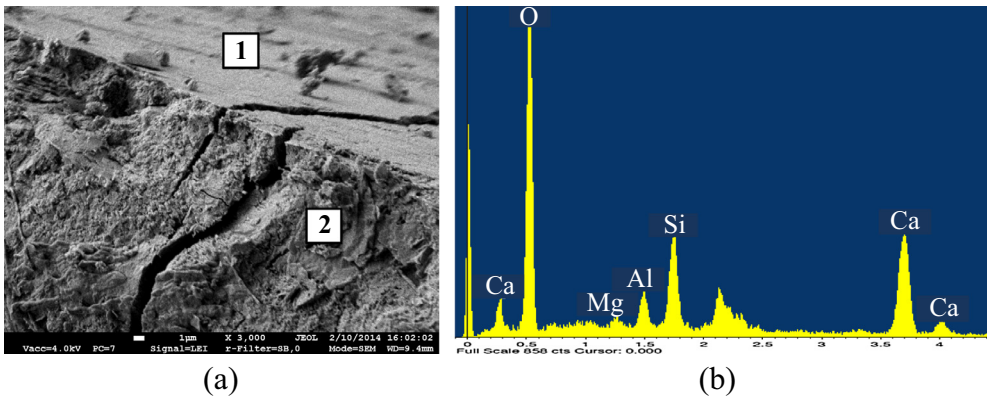

Fig. 18. Results of EDS analysis of specimen from the middle of used sleeper at the interface between reinforcement and concrete: a – image of EDS analysis (×5000) (1 – interface between reinforcement and concrete; 2 – concrete), b – results of element concentration (%): O – 53.58; Al – 1.58; Si – 6.41; Ca – 36.18; Mg – 2.26.

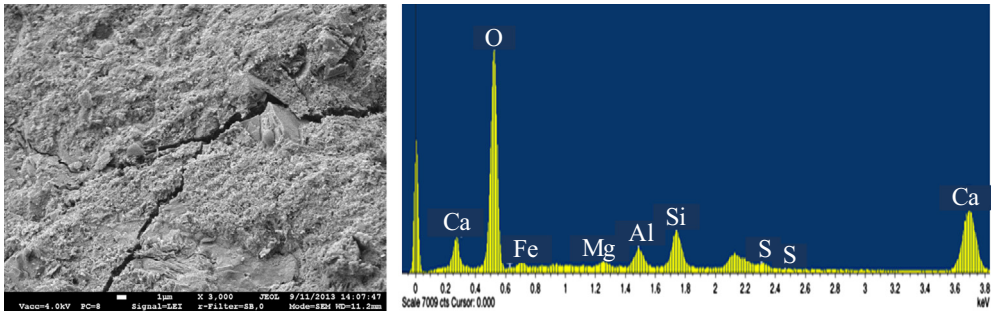

Fig. 19. Results of EDS analysis of concrete specimen from the middle of new sleeper: a – image of EDS analysis (×3000), b – results of element concentration (%): O – 55.89; Mg – 0.62; Al – 2.23; Si – 5.10; S – 0.50; Ca – 27.47; Fe – 8.20.

New solid phases were not observed in the damaged concrete structure at the ends of new sleepers (Fig. 19). According to SEM images the cracks having a width of 0.2–0.8 μm are visible at the interface between coarse aggregate and cement paste (Fig. 19a).

EDS and SEM analysis indicates that no new solid phases that could cause expansion formed in concrete micro-cracks of new prestressed concrete sleepers. Secondary ettringite crystals, that can cause the deterioration of concrete structure have formed at the ends of use prestressed concrete sleepers. However, one reason of deterioration cannot be excluded due to the fact that prestressed concrete sleepers are influenced by a number of factors affecting the durability of the sleepers during production and service in the natural environment. One factor of effect can be the beginning of another. Therefore, the behaviour and cause of the deterioration of prestressed concrete sleepers, under difficult service conditions, must be assessed in complex.

4. Conclusions

A theoretical and experimental analysis of prestressed concrete constructions, with pretensioning reinforcement to abutments, has showed that internal stresses are induced in elements during concrete heat treatment. The maximum stresses occur after hardening of concrete. Reinforcement is pulled out of concrete at the ends of the last elements in the casting bed at the cooling stage and draws into concrete during release. Reinforcement draw in depends on the method of release. Damage to the interface between reinforcement and the concrete of prestressed concrete elements at the active end of the casting bed are larger than that to other produced elements.

The damaged areas of the interface between reinforcement and the concrete of prestressed concrete sleepers in service enables moisture and aggressive substances penetrate into concrete resulting in the formation of various solid phases and ice causing internal stresses.

Laboratory tests on new sleepers cut in half have showed that structural damage to the interface between reinforcement and concrete at the natural structural end are larger than that at the cut end after 200 freezing and thawing cycles. The reinforcement surface is corroded up to 23 mm at the natural structural end of these sleepers and up to 5 mm at the cut end. The reinforcement surface corroded up to 5 mm in the sleepers stored in warehouse for three years.

Reinforcement corrosion was developed further into concrete at the uncracked ends of three year old used sleepers rather than in the new ones and reached up to 40 mm.

The amount of alkali (Si) and the content of sulphates (Al and S) were reduced at the ends of the used sleepers comparing to the new ones. S and Al with O and Ca in concrete and water from the outside form sulphate compounds and needle-shaped crystals (DEF) grow up in opened concrete micro-cracks and at the damaged interface between reinforcement and concrete.

New solid phases (crystals) were not detected in closed concrete micro-cracks (having no contact with the environment) in the middle of new and used sleepers. This indicates that sleeper resistance to environmental effects decreases because of the damaged interface between reinforcement and concrete at the ends of the sleeper during production.

The deterioration of concrete structure in the reinforcement anchorage zone of prestressed concrete sleepers appears because of the formation of secondary ettringite crystals, which causes additional stresses in concrete structure and sums with stresses induced by technological factors, environmental effects (freezing water) and external forces.

Acknowledgement

Authors are grateful to Civil Engineering Scientific Research Centre of Vilnius Gediminas Technical University and Laboratory of Building Products Technology in the Scientific Institute of Thermal Insulation, Vilnius Gediminas Technical University for equipment and infrastructure, which were employed for investigation.

References

[1] P. Okumus, M.G. Oliva, Evaluation of crack control methods for end zone cracking in prestressed concrete bridge girders, PCI J. 58 (2) (2013) 91–105.
[2] J. Kannel, C. French, H. Stolarski, Release methodology of strands to reduce end cracking in pretensioned concrete girders, PCI J. 42 (1) (1997) 42–54.
[3] J.F. Mirza, M.E. Tawfik, End cracking in prestressed members during detensioning, PCI J. 23 (2) (1978) 66–78.
[4] C.J. Hasenkamp, S.S. Badie, K.E. Hanna, M.K. Tadros, Proposed evaluation and repair procedures for precast, prestressed concrete girders with end-zone cracking, PCI J. 57 (2) (2012) 94–119.
[5] M.F. Stocker, M.A. Sozen, Investigation of Prestressed Reinforced Concrete for Highway Bridges, Part V: Bond Characteristics of Prestressing Strand. Bulletin 503, University of Illinois, USA, 1970.
[6] G. Marčiukaitis, Influence of Technological Factors on the Behavior of Concrete and Reinforced Concrete, Technika, Vilnius Gediminas Technical University, Vilnius, Lithuania, 2013 (in Lithuanian).
[7] N.A. Markarov, Improving the Quality of Prestressed Concrete Structures, Stroizdat, Moscow, Russia, 1984 (in Russian).
[8] P.K. Mehta, Concrete: Microstructure Properties and Materials, McGraw-Hill, New York, 2006.
[9] P. Tepponen, B.E. Eriksson, Damages in concrete railway sleepers in Finland, Nordic Concr. Res. J. 6 (1987) 199–209.
[10] M. Collepardi, Damage by delayed ettringite formation, Concr. Int. 21 (1) (1999) 69–74.
[11] M. Collepardi, A state-of-art review on delayed ettringite attack on concrete, Cem. Concr. Compos. 25 (4–5) (2003) 401–407, http://dx.doi.org/10.1016/S0958-9465(02)00080-X.
[12] S. Sahu, N. Thaulow, Delayed ettringite formation in Swedish concrete railroad ties, Cem. Concr. Res. 34 (9) (2004) 1675–1681, http://dx.doi.org/10.1016/j.cemconres.2004.01.027.

[13] K.D. Weerdt, H. Justnes, M.R. Geiker, Changes in the phase assemblage of concrete exposed to sea water, Cem. Concr. Compos. 47 (2014) 53–63, http://dx.doi.org/10.1016/j.cemconcomp.2013.09.015.
[14] W. Ferdous, A. Manalo, Failures of mainline railway sleepers and suggested remedies – review of current practice, Eng. Fail. Anal. 44 (2014) 17–35, http://dx.doi.org/10.1016/j.engfailanal.2014.04.020.
[15] A. Jokūbaitis, J. Valivonis, G. Marčiukaitis, Analysis of strain state and cracking of concrete sleepers, J. Civil Eng. Manage. 22 (4) (2016) 564–572, http://dx.doi.org/10.3846/13923730.2016.1147494.
[16] F. Rezaie, M.R. Shiri, S.M. Farnam, Experimental and numerical studies of longitudinal crack control for pre-stressed concrete sleepers, Eng. Fail. Anal. 26 (2012) 21–30, http://dx.doi.org/10.1016/j.engfailanal.2012.07.001.
[17] A.M. Remennikov, S. Kaewunruen, Experimental load rating of aged railway concrete sleepers, Eng. Struct. 76 (2014) 147–162, http://dx.doi.org/10.1016/j.engstruct.2014.06.032.
[18] H. Thun, Assessment of Fatigue Resistance and Strength in Existing Concrete Structures (Doctoral Thesis), Lulea University of Technology, Lulea, Sweden, 2006.
[19] J. Taherinezhad, M. Sofi, P.A. Mendis, T. Ngo, A review of behaviour of prestressed concrete sleepers, Electron. J. Struct. Eng. 13 (1) (2013) 1–16.
[20] H. Šimonova, V. Vesely, Z. Keršner, L. Culik, T. Mosler, V. Bilek, Influence of the age and level of concrete fatigue on prestressed railway sleeper response: parametric study and experiment, Adv. Mater. Res. 969 (2014) 218–221, http://dx.doi.org/10.4028/www.scientific.net/AMR.969.218.
[21] G. Zi, D.Y. Moon, S.J. Lee, S.Y. Jang, S.C. Yang, S.S. Kim, Investigation of a concrete railway sleeper failed by ice expansion, Eng. Fail. Anal. 26 (2012) 151–163, http://dx.doi.org/10.1016/j.engfailanal.2012.07.023.
[22] R.C. Mielenz, S.L. Marusin, W.G. Hime, Z.T. Jugovic, Investigation of prestressed concrete railway tie distress, Concr. Int. 17 (12) (1995) 62–68.
[23] A. Shayan, G.W. Quick, Microscopic features of cracked and uncracked concrete railway sleepers, ACI Mater. J. 89 (4) (1992) 348–360.
[24] C. Gonzalez-Nicieza, M.I. Alvarez-Fernández, A. Menendez-Díaz, A.E. Alvarez-Vigil, F. Ariznavarreta-Fernandez, Failure analysis of concrete sleepers in heavy haul railway tracks, Eng. Fail. Anal. 15 (1–2) (2008) 90–117, http://dx.doi.org/10.1016/j.engfailanal.2006.11.021.
[25] J. Noorzaei, P.M. Pour, M.S. Jaafar, Y.C. Fong, W.A.M. Thanoon, Numerical simulation of railway track supporting system using finite-infinite and thin layer elements under impulsive loads, J. Civil Eng. Manage. 18 (2) (2012) 245–252, http://dx.doi.org/10.3846/13923730.2012.671286.
[26] F. Bustos, P. Martinez, C. Videla, M. Lopez, Reducing concrete permeability by using natural pozzolans and reduced aggregate to paste ratio, J. Civil Eng. Manage. 21 (2) (2015) 165–176, http://dx.doi.org/10.3846/13923730.2013.802719.
[27] J. Wambach, A. Wokau, A. Hiltpold, Oxidation of stainless steel under dry and aqueous conditions: oxidation behavior and composition, Surf. Interface Anal. 34 (2002) 164–170, http://dx.doi.org/10.1002/sia.1275.
[28] N. Ranjbar, M. Mehrali, M. Mehrali, U.J. Alengaram, M.Z. Jumaat, High tensile strength fly ash based composite using copper coated micro steel fiber, Constr. Build. Mater. 112 (2016) 629–638, http://dx.doi.org/10.1016/j.conbuildmat.2016.02.228.
[29] N. Ranjbar, S. Talebian, M. Mehrali, C. Kuenzel, H.S.C. Metselaar, M.Z. Jumaat, Mechanisms of interfacial bond in steel and polypropylene fiber reinforced geopolymer composites, Compos. Sci. Technol. 122 (2016) 73–81, http://dx.doi.org/10.1016/j.compscitech.2015.11.009.
[30] G. Marčiukaitis, E. Dulinskas, The Stress and Strain State of Prestressed Reinforced Concrete Members During Steam Curing, Ministry of Higher and Special Technical Education of Lithuania SSR, Vilnius Civil Engineering Institute, Vilnius, Lithuania, 1975 (in Russian).
[31] V.S. Galvez, M. Elices, A. Erdelyi, M. Kosiorek, Stress relaxation due to steam curing, Mater. Struct. 10 (6) (1977) 351–356.
[32] M. Andersen, Monitoring of the Sleeper Production in Marijampolė – Prestress Losses and Temperature in Concrete, Abetong AB, Växjö, Sweden, 2011.
[33] M. Andersen, R. Bolmsvik, Measuring of Prestress Losses in Vislanda 2010, Abetong AB, Växjö, Sweden, 2011.
[34] B.G. Rabbat, H.G. Russell, Friction coefficient of steel on concrete or grout, J. Struct. Eng. 111 (3) (1985) 505–515, http://dx.doi.org/10.1061/(ASCE)0733-9445(1985) 111:3(505).
[35] Rilem TC 191-ARP, RILEM Recommended Test Method AAR-0. Detection of Potential Alkali-Reactivity in Concrete. Outline Guide to the Use of RILEM Methods in Assessments of Alkali-Reactivity Potential, Mater. Struct. 36 (261) (2003) 472–479.
[36] RILEM Recommended Test Method AAR-2, Detection of potential alkali reactivity of aggregates – The ultra-accelerated mortar-bar test, Mater. Struct. 33 (229) (2000) 283–289.
[37] LST EN 196-2:2013, Method of Testing Cement – Part 2: Chemical Analysis of Cement, Lithuanian Standards Board, 2013.
[38] J. Pawluk, Corrosion hazards of railway sleepers, part I, Cement Wapno Beton R.18/80, No. 3 (2014) 174–184.
[39] Z. Li, Advanced Concrete Technology, John wiley & sons Inc., New Jersey, 2011.
[40] J. Newman, B.S. Choo, Advanced Concrete Technology. Concrete Properties, Elsevier, Butterworth-Heinemann, Great Britain, 2003.
[41] LST 1974:2012, Rules for the Application of LST EN 206-1 and Additional National Requirements, Lithuanian Standards Board, 2012.
[42] B. Jonaitis, G. Marčiukaitis, J. Valivonis, Analysis of the mechanics of carbamide induced destruction of concrete and ceramic bricks, Constr. Build. Mater. 48 (2013) 917–924, http://dx.doi.org/10.1016/j.conbuildmat.2013.07.042.
[43] N. Thaulow, V. Johansen, U.H. Jakobsen, What causes delayed ettringite formation?, in: K. Scrivener, F. Young (Eds.), Mechanism of Chemical Degradation of Cement-Based Systems, E & FN Spon, London, 1997, pp. 219–226.
[44] C.D. Lawrence, Physicochemical and mechanical properties of portland cements, in: P.C. Hewlett (Ed.), Lea's Chemistry of Cement and Concrete, Elsevier Science & Technology, 2004, pp. 345–419.
[45] Report of the Thaumasite Expert Group, The Thaumasite Form of Sulphate Attack: Risks, Diagnosis, Remedial Works and Guidance on New Construction, Her Majesty's Stationery Office, London, 1999.
[46] J. Aguilera, S. Martinez-Ramirez, I. Pajares, M.T. Blanco-Varela, Formation of thaumasite in carbonates mortars, Cem. Concr. Compos. 25 (8) (2003) 991–996, http://dx.doi.org/10.1016/S0958-9465(03)00121-5.
[47] B. Slomka-Slupik, The changes of phases composition of the paste from cement CEM III/A under the influence of NH4Cl water solution, Cement Wapno Beton R.14, No. 2 (2009) 61–66.
[48] K.N. Jallad, M. Santhanam, M.D. Cohen, Stability and reactivity of thaumasite at different pH levels, Cem. Concr. Res. 33 (3) (2003) 433–437.
[49] M.E. Gaze, The effects of varying gypsum content on thaumasite formation in a cement lime sand mortar at 5 °C, Cem. Concr. Res. 27 (2) (1997) 259–265.
[50] S.A. Hartshorn, J.H. Sharp, R.N. Swamy, The thaumasite form of sulfate attack in Portland-limestone cement mortars stored in magnesium sulfate solution, Cem. Concr. Compos. 24 (3–4) (2002) 351–359.